Photoemission study of Pd and Pt impurities in and on silver

Photoemission study of Pd and Pt impurities in and on silver

H-V Roy†, F Patthey†, W-D Schneider† and B Delley‡

† Institut de Physique Expérimentale, Université de Lausanne, CH-1015 Lausanne, Switzerland
‡ Paul-Scherrer-Institut, Badenerstrasse 569, CH-8048 Zürich, Switzerland

Abstract. The electronic structures of Pd and Pt atoms adsorbed on the (110) surface of silver and of the related dilute Ag–(3 at.% Pd) and Ag–(3 at.% Pt) alloys have been studied at room temperature using photoelectron spectroscopy. The observed difference between the lineshape of the virtual bound palladium 4d (platinum 5d) state on the respective isolated atoms supported on the (110) surface and that of an impurity atom embedded in the bulk is well accounted for by a many-body calculation performed within the Anderson single-impurity model. This analysis clearly indicates stronger s–d hybridization in the bulk than at the surface, consistent with the change in coordination number.

1. Introduction

The comparison of the electronic structure of single atom impurities deposited on a noble metal surface with the structure resulting from dissolving the same impurities in the volume is interesting for experimental and theoretical studies of localization and correlation problems [1–4]. In particular, because of recent progress in the calculation of the spectral function within the Anderson single-impurity model [5–7], the observed electron distribution in a photoemission experiment can be quite successfully computed and important physical parameters such as the Coulomb correlation energy U and the hybridization strength $V^2(\epsilon)$ between the local electron state on the impurity and the conduction electron states of the substrate and/or matrix can be extracted from such an analysis.

Dilute alloys have been investigated rather frequently in the past by photoelectron spectroscopy and various theoretical models have been considered to interpret the spectroscopic results [8–13]. For dilute transition-metal impurities deposited on solid surfaces, however, the literature is much more scarce [14] and only recently has a new interest evolved in these systems in the context of a crystal growth and supported clusters [15–20]. Specifically, a recent photoemission study of Pt impurities deposited on an Ag(110) single-crystal surface revealed an anomalous virtual bound-state width of the Pt $5d_{5/2}$ spin–orbit component [21]. Calculations performed within the Anderson single-impurity model clearly show that this broadening is mainly caused by an energy-dependent coupling between the Pt 5d state and the Ag conduction band states [21]. The motivation for the present investigation is to verify whether this energy-dependent coupling also determines the interaction of Pd impurities on the same surface and to what extent the coupling strength has to be modified for dilute Pt and Pd impurities embedded in solid silver.

2. Experimental details

The photoemission measurements were carried out in a custom-built VSW class 150 electron spectrometer equipped with a Mg Kα x-ray source and a high-intensity microwave gas-discharge lamp (Gammadata) producing photons of 21.2 eV (HeI) and 40.8 eV (HeII) energy. The VUV radiation is monochromatized by a home-built monochromator, yielding satellite-free photoelectron spectra. The angular resolution of the spectrometer is ±2°; the energy resolution was chosen to be 100 meV, a compromise between an acceptable resolution and a sufficient count rate. The single-crystal Ag(110) surface was prepared by standard methods of argon ion bombardment and annealing. Within the detection limit of x-ray and ultraviolet photoemission the surface was found to be free of contaminants. Sharp low-energy electron diffraction (LEED) spots indicated a well ordered surface prior to adsorption. Pd and Pt atoms, produced by a cluster source described elsewhere [20, 22], were deposited at room temperature in the low 10^{-10} Torr range in submonolayer quantities (0.05 and 0.1 monolayer (ML)) onto the clean Ag(110) surface. Thermal energy atom scattering experiments on a similar system, Pt/Cu(110), indicate that the adatoms do not diffuse up to 330 K [23]. The dilute Ag–(3 at.% Pt) and Ag–(3 at.% Pd) alloys were prepared by melting the corresponding amounts of the constituents in an induction furnace. Subsequently the samples were annealed at 800 K for 3 days. Microprobe analysis showed good homogeneity of the alloys in the surface region within the excited volume (3 μm^3) of the technique.

3. Results and discussion

Figure 1 displays the outer-level photoelectron spectra, excited with HeI radiation and measured at normal emission, curve (a) for the clean Ag(110) surface, curve (b) at 0.1 ML Pt coverage, curve (c) at 0.1 ML Pd coverage, curve (d) for the clean polycrystalline Ag surface, curve (e) for the dilute Ag–Pt alloy, and curve (f) for the dilute Ag–Pd alloy. The spectra of clean Ag(110) and of polycrystalline Ag are in excellent agreement with those in the literature [12, 24]. We note that, owing to the present experimental set-up, no additional intensity due to a HeI satellite is present in the flat Ag sp part of the spectrum. On the other hand, the impurity-induced photoemission intensity in this part of the spectra becomes clearly visible when amplified by a factor of 10 (see figure 1). By comparison with earlier photoemission results on dilute Ag–Pt and Ag–Pd alloys these structures are identified with emission from atomic-like spin–orbit split Pt $5d_{5/2,3/2}$ and Pd $4d_{5/2,3/2}$ states [10–12]. The experimentally derived (see below) spin–orbit splittings of 1.07 ± 0.02 eV and 0.38 ± 0.04 eV are in excellent agreement with the gas-phase values for the Pt $5d^9$ and Pd $4d^9$ configurations, respectively [25]. We note two observations.

(i) The Pt $5d_{5/2}$ component (figure 1(*b*)) appears to have a linewidth twice that of the Pt $5d_{3/2}$ component.

(ii) In going from the adsorbed impurities on the Ag surface to the dilute impurities in the bulk a considerable broadening in the impurity-induced emission features occurs.

While the first observation has been analysed in detail (see above) in recent work [21], the second observation, also reported earlier for dilute Ag–Pd alloys [14], is the subject of the present investigation.

In order to quantify the observed broadening we first performed a simple lineshape analysis [26] of the Ag–Pt–Ag and Ag–Pd–Ag difference spectra, shown in figures 2(*a*) and 2(*c*) and figures 3(*a*) and 3(*c*), which are assumed to be proportional to the Pt- and
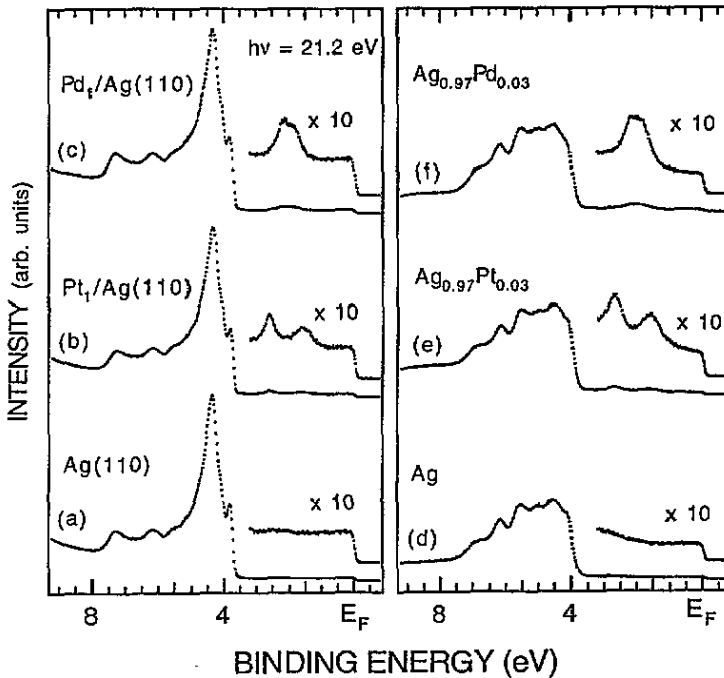
Figure 1. Outer-level photoemission spectra of clean (curve (a)), Pt-covered (0.1 ML) (curve (b)) and Pd-covered (0.1 ML) (curve (c)), Ag(110) surfaces, polycrystalline silver (curve (d)), dilute Ag–Pt alloy (curve (e)) and dilute Ag–Pd alloy (curve (f)), taken at 21.2 eV photon energy.

Pd-impurity-induced changes in the spectral function in this energy region [11]. In the first step of this analysis, two Lorentzians were used, where each was convoluted with a Gaussian of 0.1 eV FWHM to account for instrumental broadening. The Lorentzian widths were allowed to vary independently in the fit. The inelastic background was accounted for by subtracting at each point in the spectrum a value proportional to the integral intensity to the lower binding energy. When 15% occupation of a second adsorption (lattice) site at a higher binding energy is allowed for, the quality of the fit is improved. For the dilute adsorbed species, recent total-energy calculations predict the most stable adsorption site to be in the troughs of the Ag(110) surface along the [1$\bar{1}$0] direction [22]. For the dilute alloys this extra line broadening is possibly caused by alloy disorder. Including finally the possibility of crystal-field-split levels (see below) in this analysis, the result represented by the full curves in figures 2(a) and 2(c) and figures 3(a) and 3(c) is obtained. For the adsorbed impurities a spin–orbit branching ratio of 1.33 is observed, which is lower than the statistical value of 1.5 and which depends on the photon energy (He I and He II) and detection angle, indicating diffraction and photoionization cross section effects [27, 28]. Table 1 summarizes the relevant binding energies and Lorentzian linewidths obtained from this analysis for the impurity systems considered in the second to fifth columns. The spin–orbit and crystal-field splittings used in this analysis are displayed in the sixth and seventh columns, respectively. The essential result of this preliminary analysis is that the widths of the spin–orbit components observed for the dilute alloys are considerably larger than those for the adsorbed impurities. Moreover, the $j = 5/2$ components are always larger than the $j = 3/2$ components. van der Marel *et al* [11] also observed such an effect in dilute Ag–Pt alloys. They interpret the broadening in terms of an octahedral crystal-field splitting which
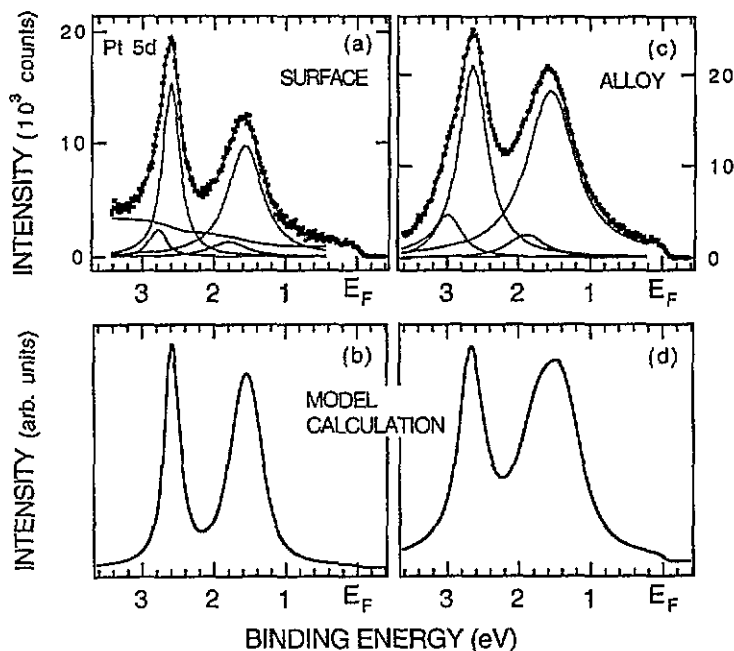
Figure 2. Pt contribution (●) (*a*) to the photoemission spectrum at 0.05 ML Pt coverage and (*c*) to the dilute alloy spectrum in figure 1, curve (*e*). The solid lines through the data represent the result of a least-squares analysis (see text). (*b*), (*d*) Spectral function of the Pt 5d excitations calculated within the single-impurity model (see text).

leads to a separation of 0.3 eV between the Γ_7 and Γ_8' states. This is a factor of 10 larger than theoretical estimates [29]. We note, however, that no crystal-field splitting (or at most a crystal-field splitting of 0.01 eV) had to be introduced to fit our dilute alloy data (0.12 eV for the supported Pt atoms) (see table 1). This discrepancy with [11] is most probably due to a data set with better statistics and higher-energy resolution in our case which permits a more reliable data analysis. Therefore, as we concluded in an earlier report on Pt impurities supported on Ag(110) [21], the crystal field alone cannot be responsible for the observed lineshapes.

The key to understanding the photoemission lineshapes in these systems is given by their peculiar electronic structure. The essential physics can be described in terms of an interaction of a localized atomic state with the delocalized conduction electrons of the substrate or of the matrix. Consequently in the energy range of the atomic bound d states there is mixing between the eigenstates of the pure systems that broadens the sharp atomic level into a resonance level, also termed the virtual bound state (VBS) [1, 2, 30]. The degree of mixing, i.e. the coupling or hybridization strength between the atomic level and the conduction band states of the metal, can be described by a hopping matrix element V^2. This leads to a broadening of the linewidth of the VBS [13]. Now, if the coupling strength $V^2(\epsilon)$ changes as a function of energy, different line broadenings are expected in different energy intervals. An example for such an energy-dependent coupling has been computed recently by Drchal *et al* [13] within a first-principles band-structure calculation. They considered a large supercell with 16 atoms where the central atom is a d impurity (Mn) surrounded by Ag atoms. They obtained a variation in the magnitude of the coupling V^2 of a factor of about 2 just in the energy range of the Ag sp band, where in our case the Pt
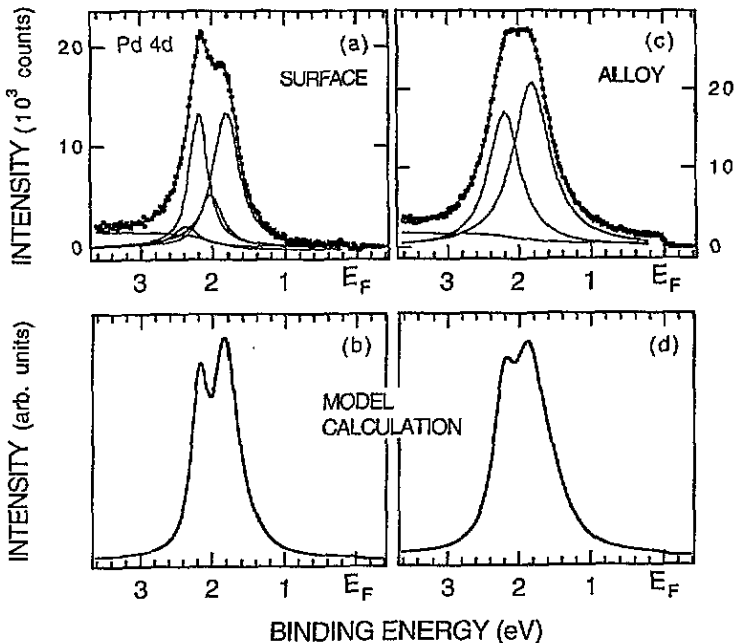
Figure 3. Pd contribution (●) (*a*) to the photoemission spectrum at 0.1 ML Pd coverage (figure 1, curve (c)) and (*c*) to the dilute alloy spectrum (figure 1, curve (f)). The solid lines for the Pd spectra and (*b*) and (*d*) are as described in the caption of figure 2.

and Pd spin–orbit doublets are located (see figure 1 of [13]).

In order to evaluate quantitatively the influence of this energy-dependent coupling on the photoemission spectra of the d impurities in and on silver we calculate within the single-impurity model of Anderson [2, 5, 7, 13] the spectral function for the 4d and 5d excitations. The ground state is modelled by a linear combination of basic states:

(i) a conduction band with no hole in the tenfold degenerate d level and

(ii) one hole in the d level and an additional electron in the conduction band above the Fermi energy E_F.

To obtain the photoemission spectrum we use a similar basis set with one electron less. Neglecting the d^8 configuration, we set the Coulomb interaction U between two holes to infinity. The coupling $V^2(\epsilon)$ in the energy range of interest is chosen to be similar to that in [13] in our model calculation. Its energy dependence is simulated here by a superposition of two Lorentzians with different linewidths. The energy position $\epsilon_{d_{3/2}}$ of the uncoupled (without interaction with the Ag conduction band) hole state and the strength V^2 (see table 1, eighth and ninth columns, respectively) were varied until best agreement between the computed spectral functions and the photoemission spectra was obtained. The corresponding energy-dependent coupling V^2 is displayed in figure 4 and its maximum value is reported in table 1, ninth column. The spin–orbit splittings and crystal-field splittings used in the calculation are displayed in the sixth and seventh columns, respectively, of table 1, where in the latter case the degeneracies due to octahedral symmetry are adopted [11, 21]. With these parameters the many-body calculation yields hybridization-induced energy gains of the d levels and ground-state occupations n_d for the d shells in the different systems, displayed in the tenth and eleventh columns of table 1. Since photoionization cross section

Table 1. Experimental (least-squares analysis) UPS impurity peak maxima E_B, full widths Γ at half-maximum, spin–orbit splitting Δ_{SO} and cubic crystal-field splitting $E_{\Gamma'_8} - E_{\Gamma_7}$. The parameters that were used in the single-impurity calculation of the spectral function are Δ_{SO}, $E_{\Gamma'_8} - E_{\Gamma_7}$, the position $\epsilon_{d_{3/2}}$ of the uncoupled d level and the maximum value of the hopping matrix element $V^2_{max}(\epsilon)$ (see figure 4). The parameters which result from the single-impurity calculation are the energy gain δ in the ground state due to hybridization and the ground-state occupancy n_d of the d shell.

	E_B ($d_{5/2}$) (eV)	E_B ($d_{3/2}$) (eV)	Γ ($d_{5/2}$) (eV)	Γ ($d_{3/2}$) (eV)	Δ_{SO} (eV)	$E_{\Gamma'_8} - E_{\Gamma_7}$ (eV)	$\epsilon_{d_{3/2}}$ (eV)	$V^2_{max}(\epsilon)$ (eV)	δ (eV)	n_d
Pt/Ag(110)	1.53 ± 0.01	2.60 ± 0.01	0.53 ± 0.01	0.24 ± 0.01	1.07 ± 0.02	0.12	2.16	0.062	0.40	9.88
Pd/Ag(110)	1.81 ± 0.02	2.19 ± 0.02	0.39 ± 0.03	0.28 ± 0.08	0.38 ± 0.04	0.01	1.72	0.062	0.40	9.89
Ag–Pt	1.55 ± 0.01	2.64 ± 0.01	0.79 ± 0.01	0.45 ± 0.01	1.09 ± 0.02	0.01	1.60	0.162	1.02	9.74
Ag–Pd	1.82 ± 0.01	2.20 ± 0.01	0.59 ± 0.01	0.50 ± 0.01	0.38 ± 0.02	0	1.45	0.112	0.71	9.81

and diffraction effects are not accounted for in our model calculation, the experimentally observed branching ratios of 1.3 cannot be simulated. However, apart from this restriction we note that the calculated spectral functions for the d excitations, shown in figures 2(*b*) and 2(*d*) and figures 3(*b*) and 3(*d*), convincingly reproduce the essential features, i.e. the energy positions and the linewidths of the observed spectra.
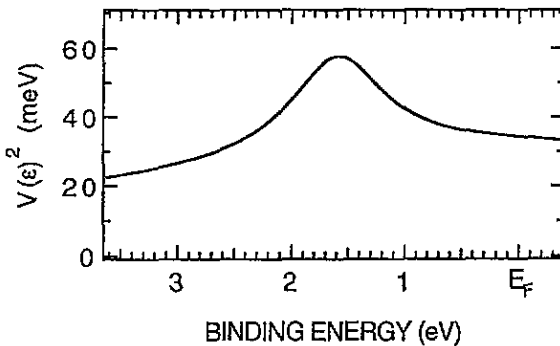

Figure 4. Energy-dependent hopping matrix element $V^2(\epsilon)$ used in the calculation for the spectral functions displayed in figures 2(*b*) and 2(*d*) and figures 3(*b*) and 3(*d*). The strength shown corresponds to Pt/Ag(110).

For all systems the same shape of V^2 as shown in figure 4 has been used but, depending on the individual coupling strengths, the actual values found are those reported for $V^2_{max}(\epsilon)$ in table 1. As it is evident from this table, for Pd/Ag(110) and for Pt/Ag(110) [21] identical hybridization strengths are found. For the alloy systems, however, the strength of V^2 had to be increased considerably in order to obtain agreement with experiment. Starting from the hypothesis that V^2 should be proportional to the overlap of the outer wavefunctions, to a first approximation it should be proportional to the number of nearest Ag atoms. At the Ag surface, Pt and Pd have five neighbours; in the dilute alloys (FCC) there are 12, i.e. V^2 should increase by a factor of 2.4 in the dilute alloy. The calculations yield 2.6 for Pt and 1.8 for Pd (cf table 1) which is surprisingly close to expectations. It is interesting to compare this result with what has been obtained in an earlier study of Pd impurities on Ag(100) and in Ag [14]. Also considerable line broadening in going from the supported impurity to the embedded impurity was observed. The Lorentzians due to the s–d hybridization increase from 0.3 to 0.5 eV FWHM which is in good agreement with our values (cf table 1).

With increasing hybridization the d occupation n_d decreases (see table 1) so that in going from the adsorbed Pt (Pd) impurity to the dilute alloy impurity we obtain a change in n_d from 9.88 (9.89) to 9.74 (9.80). This trend is in agreement with theoretical expectations where Pt (Pd) metal has a d occupancy of 9.06 (9.41) electrons [31]. Finally, the calculated spectral function shows a weight transfer to the lower-lying d component due to hybridization, thus changing the branching ratio from the atomic value of 1.5 to about 2. The measured spectra display the opposite trend. This discrepancy is most probably due to the combined action of photoelectron diffraction and of energy-dependent photoionization cross section changes as well as to the limitations of the model.

4. Summary

For Pt and Pd impurities in silver and on Ag(110) single-crystal surfaces the formation of virtual bound d states has been observed by photoelectron spectroscopy and has been simulated successfully by many-body calculations within the Anderson single-impurity model. This analysis clearly accounts for the observed lineshape changes in the different systems and determines quantitatively the increase in s–d hybridization for bulk impurities compared with supported impurities, consistent with the change in coordination number. These results may stimulate further applications of the combination of high-resolution photoemission with powerful computing techniques for the investigation of the electronic structure of condensed matter in the bulk and at surfaces.

Acknowledgments

References

[1]   Friedel J 1958 *Nuovo Cimento Suppl.* **7** 287
[2]   Anderson P W 1961 *Phys. Rev.* **124** 41
[3]   Grüner G and Zawadowski A 1974 *Rep. Prog. Phys.* **37** 1497
[4]   Bosch A, Feil H, Sawatzky G A and Julianus J A 1984 *J. Phys. F: Met. Phys.* **14** 2225
[5]   Gunnarsson O and Schönhammer K 1983 *Phys. Rev.* B **28** 4315; 1983 *Phys. Rev. Lett.* **50** 604; 1987 *Handbook on the Physics and Chemistry of Rare Earths* vol 10 ed K A Gschneidner, L Eyring and S Hüfner (Amsterdam: North-Holland) ch 64
[6]   Keiter H and Quinn Q 1990 *Physica* B–C **163** 594
[7]   Patthey F, Imer J M, Schneider W D, Beck H, Baer Y and Delley B 1990 *Phys. Rev.* B **42** 8864
[8]   Seib D H and Spicer W E 1968 *Phys. Rev. Lett.* **20** 1441
[9]   Norris C and Nilsson P O 1968 *Solid State Commun.* **6** 649
[10] Hüfner S 1979 *Photoemission in Solids (Topics in Applied Physics 27)* ed L Ley and M Cardona (Berlin: Springer) p 173
[11] van der Marel D, Sawatzky G A and Julianus J A 1984 *J. Phys. F: Met. Phys.* **14** 281
[12] van der Marel D, Julianus J A and Sawatzky G A 1985 *Phys. Rev.* B **32** 6331
[13] Drchal V, Gunnarsson O and Jepsen O 1991 *Phys. Rev.* B **44** 3518
[14] Smith G C, Norris C, Binns C and Padmore H A 1982 *J. Phys. C: Solid State Phys.* **15** 6481
[15] Fujimori A, Grioni M, Joyce J J and Weaver J H 1985 *Phys. Rev.* B **31** 8291
[16] Colbert J, Zangwill A, Strongin M and Krummacher S 1983 *Phys. Rev.* B **27** 1378
[17] Raaen S and Strongin M 1985 *Phys. Rev.* B **32** 4289
[18] Cini M, De Crescenci M, Patella F, Motta N, Sastry M, Rochet F, Pasquali R, Balzarotti A and Verdozzi C 1990 *Phys. Rev.* B **41** 5685
[19] Kuhrt C and Harsdorff M 1991 *Surf. Sci.* **245** 173
[20] Fayet P, Patthey F, Roy H V, Detzel T and Schneider W D 1992 *Surf. Sci.* **269/270** 1101
[21] Roy H V, Boschung J, Fayet P, Patthey F, Schneider W D and Delley B 1993 *Phys. Rev. Lett.* **70** 2653
[22] Roy H V, Fayet P, Patthey F, Schneider W D, Delley B and Massobrio C 1994 *Phys. Rev.* B **49** 5611
[23] Hugenschmidt M B and De Beauvais C 1994 *Surf. Sci.* at press
[24] Roloff H F and Neddermeyer H 1977 *Solid State Commun.* **21** 561
[25] Radzig A A and Smirnov B M 1985 *Reference Data on Atoms, Molecules and Ions* (Berlin: Springer)
[26] Mahowald P H, Friedman D J, Carey G P, Bertness K A and Yeh J J 1987 *J. Vac. Sci. Technol.* A **5** 2982
[27] Margaritondo G, Rowe J E and Christman S B 1979 *Phys. Rev.* B **19** 2850
[28] Patthey L, Bullock E L and Hricovini K 1992 *Surf. Sci.* **269/270** 28
[29] Smith N V 1974 *Phys. Rev.* B **9** 1365
[30] Gadzuk J W 1974 *Surf. Sci.* **43** 44
[31] Harrison W A 1980 *Electronic Structure and the Properties of Solids* (San Francisco, CA: Freeman) p 498